Reactions of Laser-Ablated Cobalt Atoms with O_2. Infrared Spectra of Cobalt Oxides in Solid Argon

George V. Chertihin, Angelo Citra, and Lester Andrews*

Department of Chemistry, University of Virginia, Charlottesville, Virginia 22901

Charles W. Bauschlicher, Jr.*

STC-230-3, NASA Ames Research Center, Moffett Field, California 94035

Received: June 20, 1997[⊗]

Laser-ablated Co atoms react with O_2 to give the linear dioxide, the monoxide, and the rhombic $(CoO)_2$ dimer molecules. The linear OCoO molecule is characterized by oxygen-18 substitution in strong ν_3 (945.4 cm^{-1}) fundamental and weak $\nu_1+\nu_3$ (1717.6 cm^{-1}) combination bands. Annealing to 20−30 K to allow diffusion and reaction of cold cobalt atoms and dioxygen markedly increases weak bands due to the $Co(O_2)$ and CoOO complexes and higher species including OOCoO, $OOCoO_2$, $(O_2)CoO_2$, and the dimer $(CoO_2)_2$. DFT and CASSCF calculations performed on the three CoO_2 isomers and rhombic $(CoO)_2$ support these assignments; DFT calculations are also presented for the rhombic $(FeO)_2$ molecule.

Introduction

Reactions of transition metals with oxygen in inert matrixes have been studied for several decades. Thermal experiments provided only products of exothermic reactions, and in the case of Fe and Ni only $Fe(O_2)$ and $Ni(O_2)$ molecules were detected as initial reaction products.[1−6] Recent investigations of laser-ablated Fe and Ni atom reactions with oxygen have shown that dioxides OMO and monoxides MO can be also formed in these systems due to excess energy in the laser-ablated metal atoms.[7−9] Further annealing leads to the formation of many products, which gives rich chemistry in these systems in comparison with thermal experiments. Matrix experiments using the hollow cathode sputtering technique observed the CoO molecule[10] at 846.4 cm^{-1}. In the iron−cobalt−nickel group, cobalt has been the least studied, and gas-phase investigations[11−14] have revealed the CoO fundamental[13] at 851.7 cm^{-1} and a bond length[14] of 1.629 Å. Recent theoretical calculations found a $^4\Delta$ ground state with a 909 cm^{-1} fundamental,[15] which agrees with the experimental results. Electron spin resonance studies of laser-ablated Co atoms reacting with O_2 have found evidence for a linear OCoO dioxide in the $^2\Sigma$ ground state.[16]

The similarity of Fe, Co, and Ni metal chemistry kindles our interest in this system. Three different MO_2 isomers[7−9] were found for Fe and Ni and such is also expected for Co. The FeOO isomer is of interest for comparison to asymmetric superoxo absorptions in Fe(II) porphyrins and oxyhemoproteins,[17,18] and the CoOO isomer is expected to be similarly related to the analogous Co(II) compounds.[19,20] New cobalt oxides obtained in this work are of chemical interest as they may serve as intermediates in different processes involving corrosion and electrochemistry of alloy materials.

Experimental Section

The technique for laser ablation and FTIR matrix investigation was identical with that employed previously.[7−9] Cobalt (Johnson-Matthey, 99.9+%) was used for the laser target. Oxygen samples (Matheson, Yeda 55% and 99% ^{18}O) were used as received. Typical matrix dilution was 0.2−1% in argon and nitrogen, although experiments with higher and lower concentrations were also done. Gas mixtures were codeposited 1−2 h on cooled (10 ± 1 K) CsI window at 2−6 mmol/h with ablated Co atoms using 20−40 mJ pulses of 1064 nm radiation from a Nd:YAG laser. Annealing and photolysis by a medium-pressure mercury arc (Philips, 175 W) with globe removed (240−580 nm) were also done. FTIR spectra were recorded with 0.5 cm^{-1} resolution on a Nicolet 750 spectrometer.

Results

Matrix FTIR spectra of the laser-ablated Co + O_2 reaction system will be presented.

Co + O_2/Ar. The spectra of Co ablated at 40 mJ/pulse and reacted with 1% O_2 in argon during condensation at 10 K are presented in Figure 1; new product absorptions are listed in Table 1. The relative yield of product bands depended more on oxygen concentration than laser power. Deposition revealed weak absorptions at 1717.6, 1286.8, 984.9, and 846.2 cm^{-1} and strong bands at 945.4, 685.2, and 469.6 cm^{-1} (Figures 1a and 2a). Annealing led to dramatic changes in the spectra: the appearance of new bands at 1365.3, 1331.6, 1090.0, 1042.5, 954.7, 944.0, 897.3, 859.7, 805.6, and 540.0 cm^{-1}, growth of the 1286.8 and 984.9 cm^{-1} bands, and decrease of the 1717.6, 945.4, 685.1, and 469.6 cm^{-1} bands. Several correlations in band intensities were found: two bands, 805.6 and 897.3 cm^{-1}, appeared in the high oxygen concentrated matrixes after annealing and grew in the same proportion, and the sharp 685.1 and 496.6 cm^{-1} bands tracked together. In an experiment run with 20 mJ/pulse of laser energy, the weak 1717.6 and strong 945.4 cm^{-1} bands increased 10% on the first and decreased 10% on the second annealing cycle, while the 846.2 cm^{-1} band decreased 25% and 50%, respectively.

Oxygen isotopic substitution was employed for band identification. Isotopic spectra are presented in Figures 2 and 3. The weak 1717.6 cm^{-1} band gave a triplet with statistical isotopic oxygen ($^{16}O_2$ + $^{16}O^{18}O$ + $^{18}O_2$ = 1:2:1). The intermediate component for the 1286.8 cm^{-1} band was broader than the pure isotopic components, which is typical for a partially resolved quartet. In a dilute statistical isotopic oxygen experiment (0.2% total O_2 in argon), the central band was resolved into 1253.6 and 1250.4 cm^{-1} peaks. The 984.9 and

[⊗] Abstract published in *Advance ACS Abstracts,* October 15, 1997.

S1089-5639(97)02022-7 CCC: $14.00

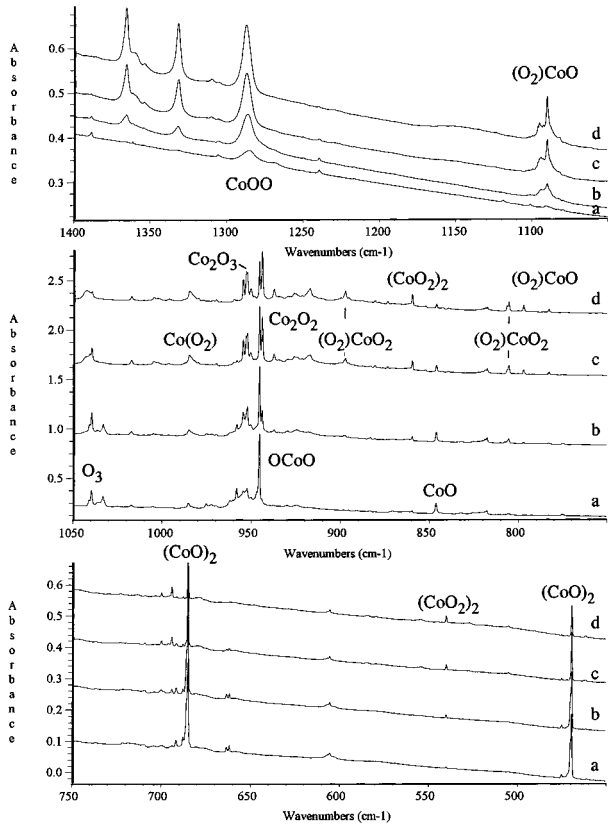

Figure 1. Infrared spectra in the 1400−1050, 1050−750, and 750−450 cm^{-1} regions (different absorbance scales) for laser-ablated cobalt atoms (higher laser energy) co-deposited with $Ar/O_2 = 100/1$ sample onto a 10 K window. (a) 2 h deposition, (b) after 20 K annealing, (c) after 30 K annealing, and (d) after annealing to 40 K.

945.4 cm^{-1} bands produced triplets on isotopic substitution with the statistical mixture and doublets with the mechanical mixture ($^{16}O_2 + {}^{18}O_2 = 1{:}1$). Other bands overlapped and many experiments were required with different conditions to find their isotopic structures. The bands at 954.7 and 944.0 cm^{-1} produced doublets of triplets, while the 846.2, 685.2, and 469.6 cm^{-1} bands produced clear doublet, triplet, and triplet isotopic structures, respectively, with the statistical isotopic mixture.

Co + N_2O/Ar. An experiment with N_2O in argon gave slightly different spectra. The 846.2 cm^{-1} band ($A = 0.15$) was 3× stronger than the 945.4 cm^{-1} band after deposition; a 852.5 cm^{-1} band was observed on deposition and grew on annealing to be much stronger than the 846.2 cm^{-1} band. Weak 685.1 and 496.6 cm^{-1} bands were also observed. The 984.9 cm^{-1} band was weaker after both deposition and annealing. The 917.0 cm^{-1} band was not observed, but the 952.5 cm^{-1} band and new 942.0 and 918.5 cm^{-1} bands were produced on deposition and increased on annealing. A weak 1017.2 cm^{-1} band was observed, and weak 1019.9 and 944.0 cm^{-1} bands appeared on annealing.

Co + O_2/N_2. The cobalt atom reaction with O_2 was also examined in condensing nitrogen, and the observations are collected in Table 2 and illustrated in Figure 4. The formation of cobalt dinitrogen complexes, cobalt nitrides, and cobalt nitride oxides was confirmed by investigation of the nitrogen system with ^{15}N substitution, which will be described in a separate report.[21] The major new absorptions include bands at 1018.8 cm^{-1} (labeled $Co(O_2)$), 978.6 cm^{-1} (labeled OCoO), 943.9 cm^{-1} (labeled $NCo(O_2)$), 856.9 cm^{-1} (labeled $NCoO_2$), 798.0 cm^{-1} (NCoO), and 706.0 cm^{-1} (labeled $(CoO)_2$) in Figure 4. Annealing markedly increased the 1018.8 cm^{-1} band, slightly decreased the 978.6 cm^{-1} band, increased the sharp 706.0 cm^{-1} absorption, and produced a new 929.1 cm^{-1} absorption. Oxygen-18 shifts were observed for all bands except CoN, as illustrated in Figure 4c and given in Table 2 along with statistical (scrambled) mixed isotopic results. All of these product bands gave the sum of $^{16}O_2$ and $^{18}O_2$ isotopic spectra in a mixed ($^{16}O_2 + {}^{18}O_2$) isotopic experiment.

Ab Initio Calculations. The ground state of Co is $^4F(3d^74s^2)$, and there is a low-lying $^4F(3d^84s^1)$ excited state. When coupled with the ground $^3\Sigma_g^-$ state of O_2, we expect the low-lying states of CoO_2 to be either doublet or quartet. The sextet states are expected to be higher in energy; this is confirmed in our calculations and therefore we do not report sextet states. We first describe the level of theory and the basis sets used in this study. We then describe the computational results for CoOO, $Co(O_2)$, OCoO, and $(CoO)_2$.

The self-consistent-field (SCF) approximation typically performs very poorly for systems containing first transition row atoms, because it neglects electron correlation and cannot account for near degeneracy effects. Density functional theory (DFT) includes electron correlation, but since it is a single reference approach it cannot fully account for near degeneracy effects. However, experience has shown[22,23] that DFT can accurately treat cases where other single techniques, such as MP2, fail. In our previous study[7,8] of FeO_2, we found the Becke−Perdew (BP)[24] and hybrid[25] B3LYP[26] functionals to work reasonably well, with each functional having advantages and disadvantages. The complete-active-space SCF (CASSCF) approach can correctly treat near degeneracy effects, but does not include extensive electron correlation. For CaO_2 we found that the CASSCF yielded frequencies that were in better agreement with experiment than the B3LYP approach.[23] However, the energy separations between the various isomers were better at the B3LYP than at the CASSCF level. Because different computational approaches have different advantages and disadvantages, for a given isomer it is not obvious which computational approach is superior. As a result of problems that arose in this study, the CASSCF and DFT approaches were employed. In the DFT studies both the B3LYP and BP functionals were used. From the similarities and differences between the results of the different methods, we are able to better predict the correct vibrational frequencies. The DFT calculations were performed with Gaussian 94,[27] while the full valence CASSCF calculations were performed with SIRIUS/ABACUS.[28]

Three basis sets were used in this work; DFT studies use small and large basis sets analogous to those used in our previous DFT studies of FeO_2[7,8] and CuO_2.[29] The small oxygen basis set is the 6-31+G* set of Pople and co-workers.[30] The small Co basis set is derived from the set optimized by Wachters;[31] contraction number 3 is used for the s and p spaces, while the d orbitals are contracted (311). The diffuse d function of Hay[32] and the two diffuse p functions of Wachters (multiplied by 1.5) are added. The large oxygen set is the 6-311+G(2df) set,[30] and the large Co basis set adds an f function (α = 1.653 494 5) to the small set. The third basis set is used in the CASSCF calculations. For oxygen, the triple-ζ valence (TZV) set of Schafer, Huber, and Ahlrichs[33] (SHA) has been supplemented with two optimized Dunning[34] d functions (2.314 and 0.645) and a diffuse p function (0.058) to describe O^-. For Co, the TZV set of SHA is supplemented with two diffuse p functions (0.141308 and 0.043402) and a (3f/2f) set of polarization functions, which is a three-term fit to a Slater type orbital (STO) with an exponent of 4.0. We note that the f function in the large set is a one term fit to the same STO. The final CASSCF basis sets are of the form (17s12p6d3f)/[6s5p3d2f]

TABLE 1: Infrared Absorptions (cm^{-1}) Produced by Reactions of Laser-Ablated Co and O_2 in Argon Condensing at 10 K

$^{16}O_2$	$^{18}O_2$	$^{16}O_2 + {}^{16}O^{18}O + {}^{18}O_2$	anneal	*R*(16/18)	assignment
1717.6	1640.2	*1717.6*, 1679.4, *1640.2*	+	1.0472	OCoO ($\nu_1+\nu_3$)
1365.3	1288.8	1329	+	1.0594	$((O_2)CoOO)$
1331.5	1256.9	1295	+	1.0594	OOCoO
1286.8	1215.0	1287.0, 1253.6, 1250.4, 1215.2	+	1.0598	CoOO
1095	1034		+	1.0590	?
1090.0	1028.8	1090.0, 1060.8	+	1.0595	$(O_2)CoO$
1042.5	985.1	1042, 1013, 985	+	1.0593	$((O_2)CoOO)$
1039.6	982.3	sextet	+,−	1.0583	O_3
1033.0	976.2	sextet	−	1.0582	O_3 site
1017.2	965.5		+	1.0535	$NNCo(O_2)$
984.9	930.9	*984.9*, 958.5, *930.9*	+	1.0580	$Co(O_2)$
958.2	923.3	958.2, 943.1, 923.3	−	1.0378	OCoO site
954.7	917.2	954.7, 937.4, 917.2	+	1.0403	$OOCoO_2$ (ν_3)
953.8	901.8	isotopic dilution	−	1.0576	O_4^-
952.5	912.5	*952.3*, 950.3, *948.6*, 917.7, *914.5*, *912.6*	+	1.0438	OCoOCoO
945.4	911.1	*945.4*, 930.5, *911.1*	+,−	1.0376	OCoO (ν_3)
944.0	900.6	*944.0*, 942.6, 901.3, *900.6*	+	1.0482	CoOCoO bent
937.4	894.4	isotopic dilution	+	1.0481	site ?
917.0	874.9	isotopic dilution	+	1.0481	aggregate ?
897.3	862.2	897.3, 883.0, 862.2	+	1.0407	$(O_2)CoO_2$ (ν_3)
880.7	832.4	isotopic dilution	+	1.0580	?
859.6	824.5	*859.6*, 859.1, 858.3, 834.8, *833.4*, 832.0, 826.3, 825.3, *824.5*	+	1.0426	$(CoO_2)_2$
852.5		in N_2O experiment	+		NNCoO
846.2	808.6	846.2, 808.6	−	1.0465	CoO
817.7	784.0	isotopic dilution	+,−	1.0430	$(O_2)CoO$
805.6	763.7	805.6, 782.2, 763.7	+	1.0549	$OOCoO_2$ (ν_1)
797.3	758.3	797.3, 776.6, 758.3	+	1.0514	$(O_2)CoO_2$ (ν_1)
783.0	749.9	dilution	+	1.0441	$(O_2)CoO$
775.4	744.6	dilution	−	1.0414	?
685.2	655.2	703.0, *685.2*, 661.9, *655.2*	−	1.0458	$(CoO)_2$
605.6	580.8	dilution	−	1.0427	? Co_xO_y
540.0	512.3	*540.0*, 538.2, 533.2, *531.7*, 530.4, 516.1, 514.0, *512.3*	+	1.0541	$(CoO_2)_2$
503.1	480.0		−	1.0481	? Co_xO_y
469.6	449.0	*469.6*, 465.8, *449.0*	−	1.0459	$(CoO)_2$

[a] Italic bands observed with $^{16}O_2+{}^{18}O_2$ mixture.

for Co and (11s7p2d)/[5s4p2d] for oxygen. The CASSCF basis set is of about the same quality as the large set used in the DFT calculations.

At the top of Table 3, we compare computed results with experiment[10,11] for the X $^3\Sigma_g^-$ state of O_2 and the X $^4\Delta$ state of CoO. For CoO we also compare with previous high-level calculations.[15] For O_2, all levels of theory are in reasonable agreement with experiment; the CASSCF is too small because it does not include extensive electron correlation. For CoO, the agreement between the DFT and experiment is very good. In fact, these simple approaches are in better agreement with experiment than the previous high-level calculation. This shows the complexity of performing accurate calculations on these systems and the very good results that can be obtained using DFT methods. The CASSCF frequency is too small and the error is larger than for O_2, because electron correlation is even more important for obtaining an accurate description of CoO. However, the CASSCF treatment is expected to be more accurate in those cases where more and stronger bonds are formed; hence, this is expected to be an upper bound to the errors in the CASSCF description. We should note that the neglect of extensive electron correlation in the CASSCF approach results in sextet states incorrectly being below the X $^4\Delta$ state. Thus, while the CASSCF can be used to compute the frequencies, it is not reliable for determining the relative ordering of the states.

CoOO is the most straightforward of the systems studied. At all three levels of theory the $^2A''$, $^4A'$, and $^4A''$ states collapse to a C_{2v} $Co(O_2)$ structure, with only the $^2A'$ state having a CoOO structure. The structure is similar at all levels of theory (see Table 3). The frequencies are also in good agreement, especially if one accounts for the fact that the CASSCF frequency for free O_2 is 134 cm^{-1} lower than at the B3LYP level. The DFT approaches in the small basis set yield intensities that differ from those obtained using the CASSCF or B3LYP/large basis set approaches. Thus it appears that the intensities are somewhat sensitive to basis set.

For $Co(O_2)$ at the CASSCF level the $^4A_1$, $^4B_1$, $^4B_2$, and $^4A_2$ states are all within 830 cm^{-1} of each other and have similar vibrational frequencies (see Table 3). The analogous doublet states are significantly higher in energy, but like the quartet states, the four doublet states are close to each other in energy and the frequencies are very similar. At the B3LYP level, the doublet states are lower lying than at CASSCF because lower spin states tend to have more electron correlation than higher spin states. In fact, it is not possible to definitively predict if the ground state is doublet or quartet, without comparison to experiment. At the B3LYP level, the $^4A_1$ state is the lowest, followed by the $^4B_1$ state. In addition to lowering the doublet states, the addition of electron correlation at the B3LYP level leads to a larger variation in the vibrational frequencies. The CASSCF is expected to underestimate any ionic contribution to the bonding, so the B3LYP results are expected to be more accurate. As a minimum the B3LYP results suggest that improved treatments will reduce the frequency of the higher CASSCF a_1 mode. The BP result is different from either the CASSCF or B3LYP results, as it predicts a doublet ground state. However, the b_2 mode has a high frequency and intensity that suggests a symmetry-breaking problem. The symmetry breaking is even more pronounced in the quartet states, where the two Co−O bond lengths become unequal. Thus it appears that BP is unable to treat this structure reliably.

The last CoO_2 structure considered is OCoO. At all levels of theory the doublet and quartet states are close in energy. On the basis of the ESR experiment[16] that has been interpreted as showing that the ground state is $^2\Sigma_g^+$, at least in the matrix, we

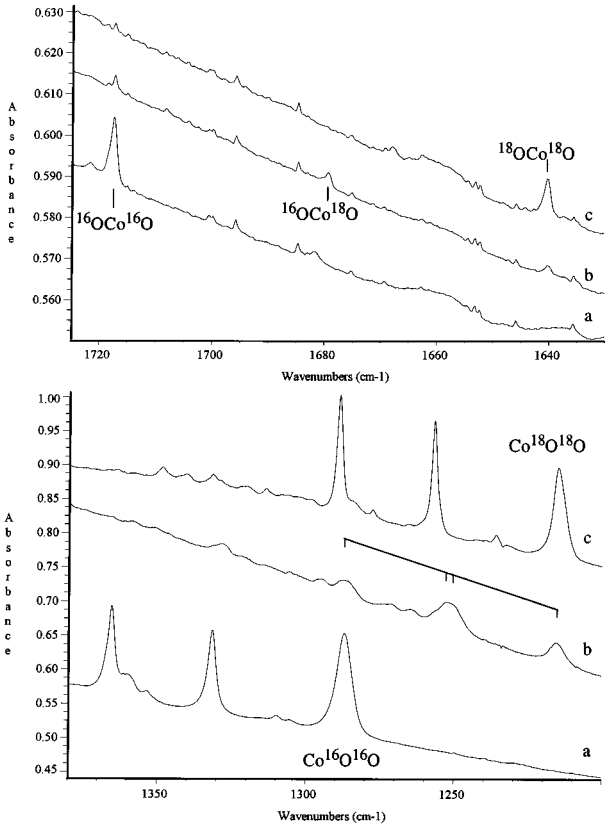

Figure 2. Infrared spectra for laser-ablated cobalt atoms co-deposited with 1% oxygen isotopic samples in argon in the 1720−1630 cm^{-1} region after sample deposition onto 10 K substrate and the 1380−1200 cm^{-1} region after annealing to 40 K: (a) $^{16}O_2$, (b) $^{16}O_2 + {}^{16}O^{18}O + {}^{18}O_2 = 1:2:1$, and (c) $^{18}O_2$. Note weak water vibration−rotational line contribution ($A = 0.002$) at 1717.6 cm^{-1}.

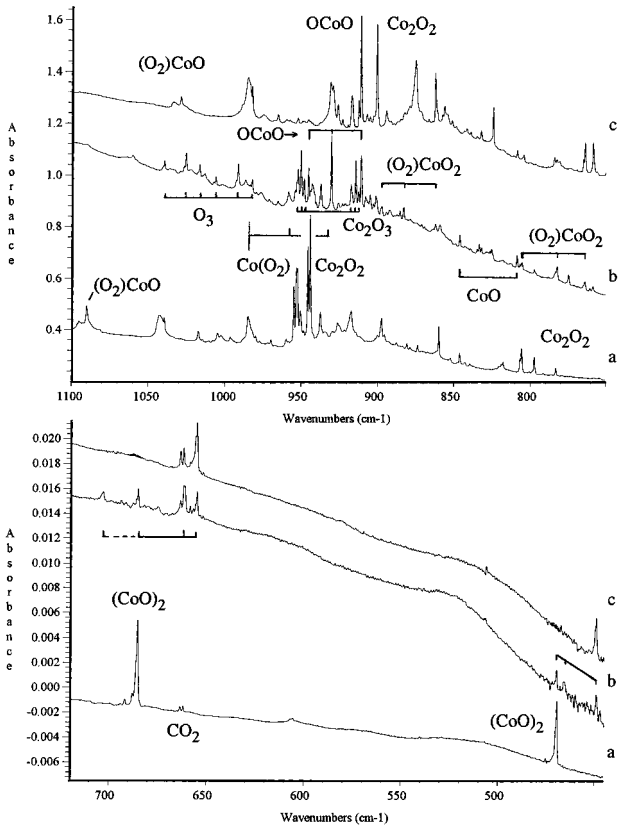

Figure 3. Infrared spectra for laser-ablated cobalt atoms co-deposited with isotopic O_2 samples (1%) in argon in the 1100−750 cm^{-1} region after annealing to 40 K and in the 700−450 cm^{-1} region after deposition onto 10 K substrate: (a) $^{16}O_2$, (b) $^{16}O_2 + {}^{16}O^{18}O + {}^{18}O_2 = 1:2:1$, and (c) $^{18}O_2$.

focus on the doublet states. For the BP and B3LYP approaches, the $^2\Sigma_g^+$ state is the lowest linear doublet state. At the CASSCF level, the $^2\Delta_g$ state is the lowest, with the $^2\Sigma_g^+$ being 1487 cm^{-1} higher. This separation is sufficiently small that the order of the states could be reversed with the addition of electron correlation, as demonstrated by the BP results, where the $^2\Delta_g$ state is about 7000 cm^{-1} above the $^2\Sigma_g^+$ state. At both the B3LYP and BP levels, the $^2\Sigma_g^+$ state has an imaginary frequency and becomes bent with an angle in the range 141−152°, depending on functional and basis set. In addition to bending, B3LYP yields inequivalent Co−O bond lengths. This bent structure is about 700 cm^{-1} below the linear at the B3LYP level and about 200 cm^{-1} below using the BP functional. We feel that the inequivalent bond lengths are unphysical, and we excluded the B3LYP results from further consideration. The bending at the BP level seems odd for a $^2\Sigma_g^+$ state; however it cannot be excluded from consideration, as the barrier is sufficiently low that the system could be linear in the matrix. Unlike the DFT methods, the CASSCF approach yields all real frequencies for the $^2\Sigma_g^+$ linear structure. In addition to being in agreement with the ESR results, the computed frequencies agree well with the current experiment, so we adopt the CASSCF approach as the most accurate for OCoO.

DFT calculations were also done for two higher oxide species found in the Ni/O_2 system.[9] For OOCoO, doublet, quartet, and sextet states have O−O stretching frequencies calculated 20−80 cm^{-1} higher than CoOO. Frequencies for the most stable $^6A'$ state are given in Table 4. Likewise for $(O_2)CoO$, doublet, quartet, and sextet states were found, and frequencies for the most stable $^6A_1$ state are listed in Table 4. The $(O_2)CoO$ molecule is more stable than $O_2 + CoO$ by 30 kcal/mol on the basis of DFT calculations.

Calculations were performed for $(CoO)_2$ in singlet, triplet, quintet (seven converged), and septet spin states; the higher multiplicities were more stable, and the three lowest energy structures are listed in Table 5. The calculated quintet frequencies fit as well as the septet frequencies, and the quintet states are only 7 and 27 kcal/mol higher. These $(CoO)_2$ states are strongly bound with respect to CoO; the ^7A_u $(CoO)_2$ state is more stable than 2CoO by 72 kcal/mol, for example, on the basis of DFT calculations.

Finally, DFT calculations were also done for cyclic $(FeO)_2$ in singlet, triplet, quintet, and septet spin states. The lowest energies were found for triplet and quintet states; five different electronic states were calculated for these spin multiplicities, and the lowest energy for each is given in Table 6. As will be discussed below, the two strong observed absorptions agree with the calculated triplet values within 0.8% and 4.3%, and the relative intensities are in excellent agreement.[8] Although the ^7A_u state is only 19 kcal/mol higher, the strong calculated b_{3u} mode is about half of the observed value, and the ^5A_g state calculated 27 kcal/mol higher has b_{2u} and b_{3u} modes that are 4.1% low and 13.7% high, respectively. The cyclic $^3A_2$ $(FeO)_2$ molecule is calculated to be more stable than 2FeO by 64 kcal/mol.

Discussion

The identification of reaction products and assignment of bands will be presented.

CoO. The 846.2 cm^{-1} band observed on deposition decreased on annealing and produced a doublet using mixed isotopic oxygen. The 16/18 ratio 1.0465 is very close to the calculated harmonic diatomic ratio 1.0469. This observation is in excellent agreement with the band reported earlier, namely

TABLE 2: Infrared Absorptions (cm^{-1}) from Reactions of Laser-Ablated Co and O_2 in Nitrogen at 10 K

$^{16}O_2$	$^{18}O_2$	$^{16}O_2 + {}^{16}O^{18}O + {}^{18}O_2$	anneal	16/18	assignment
2108.7	2108.7		+		$Co(N_2)_x$
2003.2	2003.2	2003.2	+,−		N_3^-
1992.4	1992.4	1992.4	+		$Co(N_2)_x$
1983.8	1983.8	1983.8	+		$Co(N_2)_x$
1874.6	1826.3	1874.6, 1826.3	−	1.0266	NO
1771.4	1735.5	1771.4, 1735.5	+	1.0208	CoNO
1657.6	1657.6	1657.6	−		N_3
1616.0	1586.4	triplet	−	1.0186	NO_2
1346.1	1310.4	1346.1, 1310.4	+	1.0272	$(Co^+)(NO^-)$
1291.2	1252.5	doublet	−	1.0309	N_2O
1284	1212		+	1.0594	CoOO
1236.9	1211.4	1236.9, 1220.5, 1211.4	−	1.0211	NO_2^-
1204.4	1178.4	1204.4, 1192.4, 1178.4	+,−	1.0220	$(Co^+)(NO_2^-)$
1172.3	1146.2	1172.3, 1157.7, 1146.2	+	1.0228	$(Co^+)(NO_2^-)$
1043	986	sextet	+,−	1.0578	O_3
1018.8	963.4	1018.8, 991.7, 963.4	++	1.0575	$Co(O_2)$
978.6	943.0	978.6, 962.7, 943.0	−	1.0378	OCoO
943.9	894.1	944, 926, 894	−	1.0557	$NCo(O_2)$
859.1	824.8	859.1, 846.2, 824.8	−	1.0416	$(NCoO_2)$
856.9	822.7	856.9, 844.0, 822.7	−	1.0416	$(NCoO_2)$
798.0	762.2	798.0, 762.2	+,−	1.0468	NCoO
795.4	795.4		+,−		$(NN)_xCoN$
792.5	748.2	sextet	−	1.0592	O_3^-
706.0	675.0	724.7, 706.0, 683.1, 675.0	+,−	1.0459	$(CoO)_2$
704.5	664.7	sextet	+,−	1.0599	O_3
571.1	571.1		+,−		$Co(N_2)_x$
521.9	520.4	doublet	+	1.0029	N_xCoO_y
494.6	472.8		+,−	1.0460	$(CoO)_2$

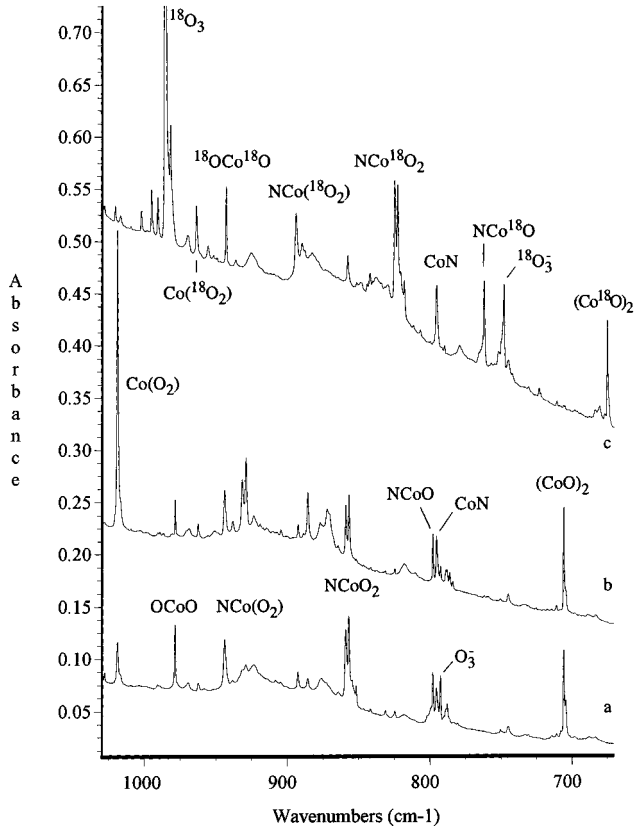

Figure 4. Infrared spectra in the 1030−670 cm^{-1} region for laser-ablated cobalt atoms co-deposited with oxygen (1%) in nitrogen on a 10 K window: (a) after co-deposition with $^{16}O_2$ for 1 h, (b) after annealing to 30 K, and (c) after co-deposition with $^{18}O_2$ for 1 h.

846.4 cm^{-1}, for cobalt monoxide in solid argon.[10] The CoO molecule can be formed by reaction 1 on the matrix surface during deposition. Although this reaction is endothermic by

$$Co + O_2 \rightarrow CoO + O \qquad (1)$$

31 ± 3 kcal/mol,[11] there is a possibility that metastable excited cobalt atoms produced in the laser ablation process[35] provide excess energy to activate reaction 1, as has been discussed for iron.[8]

The matrix assignment is in very good agreement with the recent gas-phase value,[13] 851.7 cm^{-1}, and high-level theoretical calculations for the harmonic frequency (909 cm^{-1}).[15] Note that CoO is red-shifted 5.5 cm^{-1} by the argon matrix, whereas FeO is blue-shifted 1.5 cm^{-1} and NiO is red-shifted 2.7 cm^{-1} by the solid argon medium.[7−9]

A very weak 852.5 cm^{-1} band grew on annealing, and a strong band appeared at this position with the N_2O reagent; this band, blue-shifted 6.3 cm^{-1} from CoO, is probably due to the NNCoO complex. A larger 14.5 cm^{-1} blue shift was observed for the NNFeO complex.[8]

OCoO. The sharp, strong 945.4 cm^{-1} band observed on deposition increased 10% on first annealing and decreased a like amount on second annealing in the lower laser power studies. This band gave a sharp 1:2:1 triplet with statistical oxygen isotopic substitution, which indicates two equivalent oxygen atoms. The 945.4 cm^{-1} band is the major deposition product in O_2 experiments, but the CoO band is twice as intense in N_2O experiments. The ν_3 antisymmetric stretching mode of a linear OCoO molecule has the calculated harmonic 16/18 isotopic ratio 1.0382, which nearly matches the observed 1.0376 value. A small negative anharmonicity could account for this small discrepancy. Interpretation of both the matrix ESR spectrum[16] and the photodetachment spectrum[36] of $(OCoO)^-$, which gives a strong resolved progression in ν_1 of OCoO (790 ± 60 cm^{-1}), shows that the OCoO molecule is linear. The bent (150°) iron dioxide ν_3 fundamental (945.8 cm^{-1})[8] exceeds the FeO value (872.8 cm^{-1}), and the linear nickel dioxide ν_3 mode (954.9 cm^{-1})[9] likewise exceeds the NiO value (825.7 cm^{-1}). All of the above provide a convincing case for assignment of the 945.4 cm^{-1} band to ν_3 of the linear OCoO dioxide molecule.

The sharp, weak 1717.6 cm^{-1} band tracks with the 945.4 cm^{-1} band on annealing and has 1.7 ± 0.1% of the intensity. The 1717.6 cm^{-1} band also gives rise to a sharp 1:2:1 triplet with statistical isotopic oxygen (Figure 2) and defines the 16/18 ratio 1.0472. However, this weak band is much too high for a Co−O stretching fundamental, and it must be considered

TABLE 3: Summary of Theoretical Calculations for CoO and CoO_2 Isomers[a]

Calibration Calculations

	B3LYP	BP	CASSCF	expt[b]
O_2	1641	1559	1507	1580.2

	B3LYP	BP	CASSCF	expt	ICACPF[c]
CoO	885(95)	865(65)	733(10)	846	909

CoOO (2A′ State)

method	angle	r(Co−O)	r(O−O)	a′	a′	a′
B3LY/large	111.8	1.771	1.329	92(3)	567(69)	1104(114)
B3LYP	113.7	1.860	1.307	182(7)	466(4)	1136(599)
BP	116.7	1.776	1.309	196(5)	489(5)	1140(340)
CASSCF	107.4	1.881	1.377	101(6)	552(89)	1029(47)

$Co(O_2)$

method	state	b_2	a_1	a_1	energy
B3LYP/Large	$^4A_1$	318(0.4)	436(9)	910(135)	0
B3LYP/Large	$^4B_1$	398(4)	520(3)	885(108)	566
B3LYP	$^4A_1$[d]	320(0.6)	441(7)	903(127)	0
B3LYP	$^4B_1$[d]	399(3)	514(3)	876(106)	588
B3LYP	$^4B_2$[d]	282(0.8)	476(11)	1166(119)	1070
B3LYP	$^4A_2$	393(43)	394(84)	1148(60)	6126
B3LYP	$^2B_1$	158(6)	451(30)	1129(39)	947
B3LYP	$^2B_2$	477(199)	476(21)	1155(71)	1088
B3LYP	$^2A_2$	508(39)	425(2)	1022(96)	2121
B3LYP	$^2A_1$	247(11)	355(6)	1045(135)	6315
CASSCF	$^4B_2$	327(3)	468(96)	1063(2)	0
CASSCF	$^4B_1$	338(4)	459(96)	1058(2)	51
CASSCF	$^4A_1$	294(3)	451(99)	1052(2)	507
CASSCF	$^4A_2$	279(3)	456(100)	1057(2)	830
CASSCF	$^2A_2$	201(3)	455(101)	1050(2)	4821
CASSCF	$^2B_2$	300(0.4)	471(73)	1057(0.7)	5628
CASSCF	$^2B_1$	306(0.3)	469(77)	1055(0.5)	6305
CASSCF	$^2A_1$	197(5)	456(95)	1046(1)	6529
BP	$^4A'$	226(45)[e]	546(14)	885(210)	0
BP	$^4A_1$	282i	477	887	41
BP	$^4B_1$	51i	477	896	1027
BP	$^2A_2$	1080(1508)	613(0.5)	1023(80)	−347

OCoO

method	state	angle	a_1/π	a_1/σ_g	b_2/σ_u	energy
BP	$^2A_1$	153	132(20)	992(11)	1075(174)	0
BP	$^2\Sigma_g^+$	180	74i	884	1036	145
BP	$^2\Delta_g$	180	166i	807	959	7252
BP	$^2\pi_u$	180	201(3)	720(0)	410(8)	18293
BP/large	$^2A_1$	152	132(20)	992(11)	1075(174)	0
BP/large	$^2\Sigma_g^+$	180	88i	896	1041	200
B3LYP/large	$^2A'$	141	160(31)	793(12)	994(99)	0
B3LYP/large	$^2\Sigma_g^+$	180	99i	717	908	656
CASSCF	$^2\Delta_g$	180	138(66)	611(0)	896(121)	0
CASSCF	$^2\Sigma_g^+$	180	145(98)	624(0)	896(151)	1487

[a] The frequencies and energy separations are in cm^{-1}, the intensities in km/mol, bond lengths in Å, and angles in degrees. [b] Reference 11. [c] Reference 15. [d] Although electronic transitions from the $^4A_1$ state are formally allowed, these transitions have very small calculated transition moments and are not expected to be observed in the infrared spectrum. [e] The symmetry of all vibrations for this state is a′.

for a combination band. This is clearly seen by comparing the differences, 1717.6 − 945.4 = 772.2, 1679.4 − 930.5 = 748.9, and 1640.2 − 911.0 = 729.2 cm^{-1} for each isotopic molecule. Note that the ratio of differences 772.2/729.2 = 1.0590 indicates a pure oxygen motion for the other fundamental and is appropriate for the ν_1 symmetric O ← Co → O stretching mode for a linear OCoO molecule. Therefore, the sharp, weak 1717.6 cm^{-1} band is assigned to the $\nu_1+\nu_3$ combination band for OCoO. Note that the ν_1 mode observed for OFeO (797.1 cm^{-1}) is only 15 cm^{-1} higher, and the gas-phase photodetachment[36] spectrum gives an approximate ν_1 value for OCoO (790 ± 60 cm^{-1}), which is in excellent agreement. A similar $\nu_1+\nu_3$ combination band has been observed in this laboratory for linear OPbO and bent OCrO and OVO.[37,38]

Note the matching asymmetry in the strong isotopic ν_3 and deduced ν_1 triplets. For the strong ν_3 absorption, the central $^{16}OCo^{18}O$ component is spaced 14.9−19.5 cm^{-1} from the pure isotopic values or 2.3 cm^{-1} above the mean. For the deduced ν_1 fundamental, the central component is spaced 23.3−19.7 cm^{-1} from pure isotopic values or 1.8 cm^{-1} below the mean. Clearly interaction between the two $^{16}OCo^{18}O$ fundamentals of

TABLE 4: Vibrational Frequencies, Infrared Intensities, and Structures Calculated for $(O_2)CoO$ and OOCoO by DFT[a]

	a_1	a_1	a_1	b_2	b_1	b_2
$(O_2)CoO$	1155	800	437	340	145	29
C_{2v}, $^6A_1$	(81)	(42)	(10)	(0.2)	(36)	(38)
Co−O = 1.647 Å						
Co−O_2 = 1.875 Å						
O−O = 1.339 Å						

	a′	a′	a′	a′	a″	a′
OOCoO	1177	811	481	182	89	82
C_s, $^6A'$	(444)	(46)	(2)	(0)	(76)	(26)
Co−O = 1.644 Å						
OO−Co = 1.859 Å						
O−O = 1.297 Å						
Co−O−O = 130°						

[a] The $^6A_1$ state is more stable than the $^6A'$ state by 15 kcal/mol. Frequencies (cm^{-1}) are given below mode symmetry, and intensities (km/mol) are in parentheses.

TABLE 5: Vibrational Frequencies, Infrared Intensities, and Structures Calculated by DFT for Three Low-Energy $(CoO)_2$ States of D_{2h} Symmetry[a]

	a_g	b_{2u}	b_{3u}	b_{1g}	a_g	b_{1u}
$(CoO)_2$ ^7A_u	694	646	365	431	308	130
Co−Co = 2.284 Å	(0)	(73)	(26)	(0)	(0)	(160)
O−O = 2.860 Å						
Co−O = 1.830 Å						
Co−Co = 2.406 Å $^5B_{3u}$	692	685	337	479	306	236
O−O = 2.660 Å	(0)	(12)	(7)	(0)	(0)	(72)
Co−O = 1.794 Å						
Co−Co = 2.206 Å $^5B_{1g}$	705	631	473	365	426	251
O−O = 2.861 Å	(0)	(93)	(15)	(0)	(0)	(63)
Co−O = 1.806 Å						

[a] The $^5B_{1g}$ and $^5B_{3u}$ states are 27 and 7 kcal/mol higher, respectively, than the ^7A_u state. Frequencies (cm^{-1}) given below mode symmetry, and intensities (km/mol) are in parentheses.

TABLE 6: Vibrational Frequencies, Infrared Intensities, and Structures Calculated by DFT for Three Low-Energy $(FeO)_2$ States[a]

	a_g	b_{2u}	b_{3u}	b_{1g}	a_g	b_{1u}
$(Fe^{16}O)_2$ $^3A_2$	694	655	540	437	262	208
Fe−Fe = 2.415 Å	(0.7)	(121)	(125)	(2)	(0.4)	(49)
O−O = 2.690 Å	682	635	529	427	261	203
Fe−O = 1.849 and 1.767 Å[b]	(17)	(99)	(118)	(3)	(0.4)	(47)
$(Fe^{16}OFe^{18}O)$	659	626	516	419	260	198
$(Fe^{18}O)_2$	(0.7)	(110)	(114)	(2)	(0.4)	(45)
$(Fe^{16}O)_2$ ^5A_g	689	634	588	582	308	167
Fe−Fe = 2.510 Å	(0)	(160)	(340)	(0)	(0)	(55)
O−O = 2.558 Å						
Fe−O = 1.792 Å						
$(Fe^{16}O)_2$ ^7A_u	716	711	261	219	408	182
Fe−Fe = 2.100 Å	(0)	(111)	(251)	(0)	(0)	(15)
O−O = 2.939 Å						
Fe−O = 1.806 Å						

[a] The ^7A_u state is 19 kcal/mol higher and the ^5A_g state is 27 kcal/mol higher than the lowest triplet state studied here, $^3A_2$. Frequencies (cm^{-1}) are given below mode symmetry, and intensities (km/mol) are in parentheses. [b] Distortion of this state is probably an artifact of the calculation. The mode symmetries for D_{2h} are retained.

the same symmetry gives rise to these complementary displacements. The "ν_1" mode for $^{16}OCo^{18}O$ deduced near 750 cm^{-1} was still too weak to be observed, although its presence is manifested by asymmetry in the ν_3 triplet. Finally, the observation of both ν_3 and $\nu_1+\nu_3$ modes for the linear cobalt dioxide molecule OCoO confirms this assignment.

The CASSCF calculations predict the ν_3 mode of linear OCoO to be 5% lower than observed, but the ν_1 mode 19% lower than deduced from the combination band.

Thus, in the Fe−Co−Ni group the metal dioxide valence angle increases from OFeO (150°) to OCoO (linear), and ONiO (linear) while the ν_3 fundamentals are within 950 ± 5 cm^{-1}. Finally, note that the average stretching frequency for OCoO (1717.6/2 = 858.8 cm^{-1}) is only slightly higher than the CoO value (846.2 cm^{-1}). Almost the same relationship holds for OFeO (871.5 cm^{-1} average of ν_3 and ν_1) and FeO (872.8 cm^{-1}), and for ONiO (ν_3 observed 955 cm^{-1}, ν_1 calculated scaled 748 cm^{-1}) and NiO (825.7 cm^{-1}).[8,9] Clearly Fe, Co, and Ni are capable of supporting true dioxide molecules.

$Co(O_2)$. The 984.9 cm^{-1} band was observed in experiments with high oxygen concentration, and it grew markedly on annealing. The triplet isotopic structure with 16/18 ratio 1.0580 indicates assignment of this band to cyclic $Co(O_2)$. The observation of O−O vibrations of cyclic $Fe(O_2)$ and $Ni(O_2)$ at 956 and 967 cm^{-1} is characteristic of the iron family, as these $M(O_2)$ molecules are peroxide-like rather than superoxide-like. Note the large blue nitrogen matrix shifts for both OCoO and $Co(O_2)$, and the $NNCo(O_2)$ complex in solid argon at 1017.2 cm^{-1} almost reaches the 1018.8 cm^{-1} nitrogen matrix value (Table 2). These large blue shifts contrast with red shifts for OFeO and $Fe(O_2)$ from solid argon to solid nitrogen.[39]

CoOO. The 1286.8 cm^{-1} band was weak on deposition but grew into a strong band on annealing (Figure 1), even stronger than $Co(O_2)$. Isotopic substitution produced a triplet with a broad intermediate component and the ratio 1.0591 using 1% O_2 samples. However, experiments with dilute scrambled oxygen observed a quartet 1287.0−1253.6−1250−1215.7 cm^{-1}. This isotopic pattern clearly indicates two inequivalent oxygen atoms. Note also that the bands at 1331 and 1365 cm^{-1} and their isotopic counterparts were not observed in the lowest oxygen concentration experiments. Comparing with the iron and nickel systems,[8,9] bands in the 1200 cm^{-1} region are characteristic of O−O vibrations in end-bonded MOO superoxo molecules; accordingly this band is assigned to CoOO. Two new bands at 1365.3 and 1331.5 cm^{-1} observed only after annealing must be due to higher aggregate complexes.

The comparison between the FeOO molecule and O_2 bound to Fe(II) in porphryins and oxyhemoproteins has been made[8] for the iron complexes $Fe(TTP)O_2$ and $Fe(OEP)O_2$; infrared bands in the 1100−1195 cm^{-1} range (splitting due to Fermi resonance) have been reported.[17] The analogous cobalt complexes $Co(TTP)O_2$ and $Co(OEP)O_2$ give 1278 and 1275 cm^{-1} infrared bands.[20] Thus, dioxygen bound end-on to Co(II) complexes absorbs about 100 cm^{-1} higher than the Fe(II) analogues, essentially the same relationship found in this laboratory for CoOO (1286 cm^{-1}) and FeOO (1204 cm^{-1}) in solid argon.[8]

Thus, cobalt dioxygen can exist in three isomeric forms analogous to the iron and nickel dioxygen species.[7−9] The linear isomer is the most stable product and can be formed on the matrix surface by reaction 2 involving energetic cobalt atoms from laser ablation and relaxed by the condensing matrix.[35] Only a very weak 930.5 cm^{-1} intermediate isotopic band was observed with $^{16}O_2 + {}^{18}O_2$, which means that the O + CoO combination reaction makes a minimal contribution to the yield of OCoO. Formation of the cyclic and asymmetric isomers does not require activation energy, as reaction 3 proceeds on annealing to 20−40 K. Note that no intermediate components were observed in experiments with mechanical isotopic mixtures, and the reaction of CoO and O makes only a minor contribution.

$$Co^* + O_2 \rightarrow [OCoO]^* \xrightarrow{\text{argon}} OCoO \qquad (2)$$

$$Co + O_2 \rightarrow Co(O_2) \text{ or } CoOO \qquad (3)$$

Higher Dioxygen Complexes. The 1365.3 and 1331.5 cm^{-1} bands, which appeared and grew strongly on annealing, are clearly due to superoxo (end-bound) complexes of other product species. Although their isotopic structures overlapped, triplets with 16/18 ratios 1.0594 can be identified. In like fashion, bands appeared at 1090.0 and 1042.5 cm^{-1} on annealing and gave triplets with a single intermediate component and ratios 1.0595 and 1.0583, respectively. These bands are due to peroxo (side-bound) complexes of other product molecules. Identification is complicated by the appearance of many new bands on annealing. The following tentative assignments are proposed: 1365.3 and 1042.5 cm^{-1} to $(O_2)CoOO$ and 1331.5 cm^{-1} to OOCoO. The latter has support in the observation of ONiOO at 1393.7 cm^{-1} with the strongest band calculated at 1427 cm^{-1} by DFT.[9]

Co_2O_2. Three bands 944.0, 937.4, and 917.0 cm^{-1} behaved very similarly. They appeared in the spectra *after annealing* and were stronger in experiments with high oxygen concentration and high yield of the CoO molecule. The last band was always broader than the first band. Isotopic substitution produced 16/18 ratios near 1.0482 for all three bands; the first band produced a doublet with $^{16}O_2 + {}^{18}O_2$ and a quartet with statistical isotopic oxygen, and structures for two other bands could not be resolved due to isotopic dilution. The important point is that no intermediate components around 920 and 900 cm^{-1} were observed for these bands.

The quartet identifies the vibration of one oxygen atom slightly coupled to a second inequivalent oxygen atom. Similar behavior was observed in the Ni/O_2 system, where a band at 973.9 cm^{-1}, just above ONiO at 954.9 cm^{-1}, showed a mixed oxygen isotopic quartet and nickel isotopic splittings for two metal atoms.[9] The strong 944.0 cm^{-1} band is assigned to the terminal Co−O stretching mode in a bent CoOCoO molecule. The fact that only a doublet is observed in the mixed experiment indicates that both oxygen atoms come from the same molecule, i.e., the addition of a cobalt atom to OCoO rather than a dimerization of CoO. The 937.4 cm^{-1} band is probably a site splitting of the very strong 944.0 cm^{-1} band. The broader 917.0 cm^{-1} band is probably due to a higher dioxygen complex of this species.

$(O_2)CoO$. The 1090.0 cm^{-1} band in the lower O−O stretching region appeared on annealing and exhibited a statistical oxygen isotopic triplet and 16/18 ratio (1.0595) appropriate for an O−O stretching mode. DFT calculations predict the strongest band of $(O_2)CoO$ at 1134 cm^{-1}, and accordingly the 1090.0 cm^{-1} band is assigned to $(O_2)CoO$. A similar band has been observed at 1095.5 cm^{-1} for $(O_2)NiO$.[9] The weaker 783.0 cm^{-1} band is tentatively assigned to $(O_2)CoO$. Although the Fe−O mode in $(O_2)FeO$ is blue-shifted from the diatomic FeO value,[8] the present DFT calculations for $(O_2)CoO$ suggest a red shift for the Co−O mode in $(O_2)CoO$ relative to CoO.

$OOCoO_2$. The 954.7 cm^{-1} band gives a scrambled isotopic triplet and a 16/18 ratio 1.0403 for the antisymmetric stretching mode of an obtuse bent O−Co−O linkage. Strong growth on annealing points to a complex, and the small perturbation from

linear OCoO suggests end-bonded dioxygen as the source of the perturbation. A weaker 805.6 cm^{-1} band also grows on annealing and gives an isotopic triplet with 16/18 ratio 1.0549, which is appropriate for a symmetric stretching mode of a similar O−Co−O linkage. Evidently the interaction of the oxygen molecule with OCoO has lowered the symmetry and made the symmetric sketching mode infrared active. The 954.7 and 805.7 cm^{-1} bands are assigned to $OOCoO_2$.

$(O_2)CoO_2$. The 897.3 cm^{-1} band grew on annealing and produced a triplet isotopic structure with 1.0407 isotopic ratio, which is appropriate for an antisymmetric OCoO vibration. The isotopic ratio indicates that the OCoO fragment is bent with angle approximately 130°. The same picture was observed for $(O_2)FeO_2$ molecule. The growth at 897.3 cm^{-1} on annealing, decrease in the very strong OCoO band on annealing, and absence of intermediate components in experiments with the mechanical isotopic mixture suggest the following reaction:

$$OCoO + O_2 \rightarrow (O_2)CoO_2 \qquad (4)$$

The 797.3 cm^{-1} band also increased about 10-fold on annealing and exhibited a scrambled isotopic triplet, which is complementary to the 897.3 cm^{-1} band. The 16/18 ratio 1.0514 is above the diatomic value, as expected for a symmetric O−Co−O stretching mode, and the triplet asymmetry requires coupling to a higher mode, in contrast to the 897.3 cm^{-1} band, whose triplet asymmetry requires coupling to a lower band. Thus, the 797.3 cm^{-1} band is assigned to the symmetric CoO_2 motion in $(O_2)CoO_2$, where intensity is gained in this motion from dipole change involving the $(O_2)Co$ subunit in $(O_2)CoO_2$.

Rhombic $(CoO)_2$. The 685.2 and 469.6 cm^{-1} bands produced triplets with statistical isotopic oxygen, which are indicative of two equivalent oxygen atoms, and 16/18 ratios 1.0458 and 1.0459, which are very close to the harmonic diatomic value. These two sharp bands decreased on annealing, and the relative intensities tracked within 5% in all of these experiments. This region is suitable for species with bridged M−O−M bonds, and by comparison with analogous molecules in the iron (660.6, 517.4 cm^{-1}, see below) and nickel (654.0, 481.6 cm^{-1}) systems,[8,9] these bands are assigned to the rhombic $(CoO)_2$ molecule.

Both bands showed asymmetries in the statistical oxygen isotopic triplets that require coupling to other nearby modes on symmetry lowering. Another band appears at 703.0 cm^{-1} for the $(Co^{16}OCo^{18}O)$ species that is responsible for displacement of the 661.9 cm^{-1} band below the mean of $(Co^{16}O)_2$ and $(Co^{18}O)_2$ at 685.2 and 655.2 cm^{-1}. Likewise the 465.8 cm^{-1} band is above the mean of 469.6 and 449.0 cm^{-1}, but the lower interacting band is not observed for the mixed isotopic molecule.

The $(CoO)_2$ molecule is also observed in solid nitrogen blue-shifted to 706.0 and 494.6 cm^{-1}. The upper band gave the same four-band pattern in the statistical mixed oxygen isotopic experiment (Table 2).

DFT calculations for $(CoO)_2$ predict septet and quintet rhombic ring states (Table 5) with strong b_{2u} and b_{3u} modes that are in reasonable but not perfect agreement with the observed values. The $^5B_{1g}$ state does have the b_{1g} mode below the b_{3u} mode, as required for the observed mode mixing and oxygen-isotopic triplet asymmetry, as found for the $(FeO)_2$ states. It is, however, impossible to tell which of these or another state is the $(CoO)_2$ species observed here. The ratio of the two IR active stretching mode frequencies can be used to calculate the CoOCo angle, and the data for $(CoO)_2$ give an angle of 68°. This compares fairly well with the angle of 78° in the DFT optimized structure. The force constant can also be calculated for Co−O in $(CoO)_2$ and is found to be 256 N m^{-1}. This is approximately half the size of the diatomic force constant of 531 N m^{-1}, and since the bond order in CoO is two, it follows that the Co−O bond order in $(CoO)_2$ is one.

Rhombic $(FeO)_2$. The previous Fe + O_2 spectra[8] were reexamined, and reassignment of the 660.6 cm^{-1} band, in addition to the 517.4 cm^{-1} band, to $(FeO)_2$ must be made. These bands decreased together (within 10%) on annealing in all experiments; unfortunately, the proximity to CO_2 and the extra 680.3 cm^{-1} band with statistical $^{16,18}O_2$ confused the issue.[8]

DFT calculations for $(FeO)_2$ predict a triplet (slightly distorted) rhombus to be the most stable state with strong "b_{2u}" and "b_{3u}" modes at 655 and 540 cm^{-1}. These calculated frequencies agree very well with the 660.6 and 517.4 cm^{-1} observed values. Of further importance the "a_g" and "b_{3g}" stretching modes are calculated at 694 and 437 cm^{-1}, and these modes will interact with the "b_{2u}" and "b_{3u}" modes, respectively, on symmetry lowering in the $(Fe^{16}OFe^{18}O)$ molecule. Note (Table 6) that in the $(Fe^{16}OFe^{18}O)$ molecule, the calculated highest, 682.4 cm^{-1}, band has significant intensity, and the calculated isotopic triplet (694, 682, 659 cm^{-1}) shows matching opposite asymmetry with the calculated "b_{2u}" triplet (655, 635, 626 cm^{-1}). The observed 680.3 and 638.7 cm^{-1} bands are then due to symmetric and antisymmetric ring stretching modes of $(Fe^{16}OFe^{18}O)$. For the mixed isotopic molecule, the lower band calculated at 427 cm^{-1} gains little intensity, but it does interact to produce asymmetry in the observed 517.4, 508.1, 494.8 cm^{-1} triplet assigned earlier to $(FeO)_2$.[8]

Note that the lower "a_g" stretching mode calculated at 262 cm^{-1} has a 2 cm^{-1} oxygen-18 shift. This is clearly due to the Fe−Fe stretching mode across the ring. The calculated 262 cm^{-1} Fe−Fe stretching mode is lower than the 299 cm^{-1} Fe_2 fundamental observed in the matrix resonance Raman spectrum[40] and the 300 ± 15 cm^{-1} value from the photodetachment spectrum.[41] Note also that the calculated Fe−Fe distance, 2.415 Å, is longer than the 2.06 Å value calculated at the MCSCF level[42] for Fe_2 and in the range to expect only weak Fe−Fe bonding across the $(FeO)_2$ ring. The FeOFe bond angle can be calculated in the same way as for CoOCo, and the value of 76° is close to the angle of 84° in the DFT optimized geometry.

In contrast the Co−Co bond across the $(CoO)_2$ ring is calculated to be shorter, 2.284 Å for the ^7A_u state, and the Co−Co bonding across the ring is expected to be stronger. The calculated low-frequency a_g mode at 308 cm^{-1} represents the Co−Co stretching mode and may be compared to 280 ± 20 cm^{-1} gas-phase and 290 cm^{-1} matrix values for Co_2, whose bond length, to date, is unknown.[41,43] All electron HFCI calculations have predicted a $^5\Sigma_g^+$ ground state for Co_2 with a 240 cm^{-1} frequency and 2.43 Å single-bond length.[44] As a final comparison, the rhombic $(NiO)_2$ species exhibits a calculated Ni−Ni distance and stretching frequency comparable to the Ni_2 molecule.[9]

Even though the absorbance of CoO was an order of magnitude stronger with the N_2O as opposed to the O_2 reagent, the yield of $(CoO)_2$ was higher with O_2. This suggests that the dimer is due to secondary reactions of OCoO and $Co(O_2)$ with a second cobalt atom. This mechanism is substantiated by the lack of mixed isotopic products in the $^{16}O_2 + {}^{18}O_2$ experiments. The same conclusion was reached for the analogous species in Fe and Ni reactions with O_2.[8,9] Finally, the sharp 942.0 and 918.5 cm^{-1} bands in the high CoO yield N_2O experiment may be due to CoOCoO dimers, but without oxygen-18 substitution, this assertion cannot be confirmed.

Co_2O_3. A strong 952.5 cm^{-1} band was observed after annealing in the Co + O_2 system and after deposition in the Co + N_2O system. Isotopic substitution revealed a sextet (doublet of triplets) pattern with the 16/18 ratio 1.0438. This ratio indicates that the band may belong to a terminal Co−O

vibration and the doublet of triplets isotopic structure might be associated with three oxygens, with two of them equivalent, and moreover, this isotopic distribution also suggests weak mode coupling. Thus, the leading candidate is the OCoOCoO molecule. The analogous absorption was detected in the nickel−oxygen system (962 cm^{-1}), assigned to the ONiONiO molecule,[9] and in the copper−oxygen system (995 cm^{-1}), assigned to the OCuOCuO molecule.[29]

$(CoO_2)_2$. The weak 859.6 cm^{-1} band grew after annealing. Isotopic substitution revealed seven bands, and it is clear that the broader band at 859.1 cm^{-1} is an unresolved triplet. At 0.2% O_2 concentration this band was further resolved, and the triplet of triplets listed in the table was observed. Hence the statistical mixed isotopic nonet requires the vibration of two equivalent oxygen atoms coupled to two more equivalent oxygen atoms. The 16/18 ratio 1.0426 indicates an antisymmetric O−Co−O vibration. A sharp 540.0 cm^{-1} band tracks with the sharp 859.6 cm^{-1} band on annealing and reveals eight scrambled isotopic components, and the 16/18 ratio 1.0541 indicates a symmetric O−Co−O vibration. Owing to the free radical nature of CoO_2, these bands are assigned to $O_2Co-CoO_2$. The iron−oxygen system gave a similar band at 861.5 cm^{-1}, which exhibited a isotopic nonet,[8] and is likely due to the analogous $O_2Fe-FeO_2$ molecule.[45] Two structures are possible, O_2M-MO_2 or $O(MO)_2O$ with terminal or bridge-bonded MO_2 groups; unfortunately, the present data do not allow determination of structure.

Other Absorptions. Several weaker bands that grow on annealing and cannot be identified are also indicated in the tables. These weak bands attest to the further reaction or complexation of cobalt oxide molecules on association. In the nitrogen matrix experiments, nitrogen oxides were also produced and reaction products such as CoNO and Co^+NO^- were observed.[46]

Finally, the nitrogen matrix experiments also provide N atoms and the possibility of tertiary product species as observed for iron.[39] The simplest such species, NCoO, is associated with the 798.0 cm^{-1} band, which exhibited a mixed oxygen isotopic doublet and ratio 1.0468 appropriate for a Co−O stretching mode. Using a $^{15}N_2$ matrix shifted this band to 797.8 cm^{-1}, showing that nitrogen is involved in a minor way.

Conclusions

Laser-ablated cobalt atoms react with oxygen to produce CoO, OCoO, and $(CoO)_2$ molecules as first products. Annealing forms secondary products, among them cyclic $Co(O_2)$, asymmetric CoOO, $(O_2)CoO$, Co_2O_2, OOCoO, $(O_2)CoO_2$, $OOCoO_2$, and the $(CoO_2)_2$ dimer.

Cobalt dioxygen exists in three isomeric forms, linear OCoO, cyclic $Co(O_2)$, and asymmetric CoOO, which were identified by oxygen isotopic shifts and splittings. The linear dioxide molecule can be formed only with excess energy in the metal atoms, as it requires activation energy, while the cyclic peroxo and asymmetric superoxo isomers can be formed spontaneously on annealing and reaction of cold atoms. Two isomers of Co_2O_2, rhombic $(CoO)_2$ and open bent CoOCoO, were found; Co−Co bonding is probably significant in the ring dimer and for the dimer $(CoO_2)_2$ as well.

The study of iron−cobalt−nickel atom reactions with oxygen shows very similar chemistry. The metal dioxygen species exist in three different isomeric forms. The metal dioxide is obtuse bent for OFeO[7,8] but linear for OCoO and ONiO.[9,16] It is important to note that the cyclic complexes are peroxide type rather than superoxide type on the basis of observation of the O−O fundamental in the 950 cm^{-1} region. For all three metals, rhombic $(MO)_2$ dimers were identified. The stability of dimers with metal−metal bonding across the ring probably arises from the transfer of electron density from antibonding orbitals on MO fragments to bonding orbitals in the M−M subunit, and this bonding increases in the series from Fe to Co to Ni.

References and Notes

(1) Abramowitz, S.; Acquista, N.; Levin, I. W. *Chem. Phys. Lett.* **1977**, *50*, 423.
(2) Chang, S.; Blyholder, G.; Fernandez, J. *Inorg. Chem.* **1981**, *20*, 2813.
(3) Serebrennikov, L. V. *Vestn. Mosk. Univ. Ser. 2, Khim.* **1988**, *29*, 451.
(4) Huber, H.; Ozin, G. A. *Can. J. Chem.* **1972**, *50*, 3746.
(5) Huber, H.; Klotzbucher, W., Ozin, G. A.; Vander Voet, A. *Can. J. Chem.* **1973**, *51*, 2724.
(6) Serebrennikov, L. V. *Vestn. Mosk. Univ. Ser. 2, Khim.* **1985**, *26*, 464.
(7) Andrews, L.; Chertihin, G. V.; Ricca, A.; Bauschlicher, C. W., Jr. *J. Am. Chem. Soc.* **1996**, *118*, 467.
(8) Chertihin, G. V.; Saffel, W.; Yustein, J. T.; Andrews, L.; Neurock, M.; Ricca, A.; Bauschlicher, C. W., Jr. *J. Phys. Chem.* **1996**, *100*, 5261.
(9) Citra, A.; Chertihin, G. V.; Andrews, L.; Neurock, M., *J. Phys. Chem. A* **1997**, *101*, 3109.
(10) Green, D. W.; Reedy, G. T.; Kay, J. G. *J. Mol. Spectrosc.* **1979**, *78*, 257.
(11) Huber, K. P.; Herzberg, G. *Constants of Diatomic Molecules*; Van Nostrand Reinhold: New York, 1979.
(12) DeVore, T. C.; Gallaher, T. N. *J. Chem. Phys.* **1979**, *71*, 474.
(13) Adam, A. G.; Azuma, Y.; Barry, J. A.; Huang, G.; Lyne, M. P. J.; Merer, A. J.; Schröder, J. O. *J. Chem. Phys.* **1987**, *86*, 5231.
(14) Ram, R. S.; Jarman, C. N.; Bernath, P. F. *J. Mol. Spectrosc.* **1993**, *160*, 574.
(15) Bauschlicher, C. W., Jr.; Maitre, P. *Theor. Chim. Acta* **1995**, *90*, 189.
(16) Van Zee, R. J.; Hamrick, Y. M.; Li, S.; Weltner, W., Jr. *J. Phys. Chem.* **1992**, *96*, 7247.
(17) Watanabe, T.; Ama, T.; Nakamoto, K. *J. Phys. Chem.* **1984**, *88*, 440.
(18) Hirota, S.; Ogura, T.; Appleman, E. H.; Shinzawa-Itah, K.; Yoshikawa, S.; Kitagaun, T. *J. Am. Chem. Soc.* **1994**, *116*, 10564, and references therein.
(19) Tourog, B. S.; Kitko, D. J.; Drago, R. S. *J. Am. Chem. Soc.* **1976**, *98*, 5144.
(20) Kozuka, M.; Nakamoto, K. *J. Am. Chem. Soc.* **1981**, *103*, 2162.
(21) Andrews, L.; Citra, A.; Chertihin, G. V.; Neurock, M. To be published.
(22) Bauschlicher, C. W.; Langhoff, S. R. *Spectrochim. Acta A* **1997**, *53*, 1225.
(23) Andrews, L.; Chertihin, G. V.; Thompson, C. A.; Dillon, J.; Byrne, S.; Bauschlicher, C. W. *J. Phys. Chem.* **1996**, *100*, 10088.
(24) Becke, A. D. *Phys. Rev. A* **1988**, *38*, 3098, Perdew, J. P. *Phys. Rev. B* **1986**, *33*; **1986**, *34*, 7406(E), and Vosko, S. H.; Wilk, L.; Nusair, M. *Can. J. Phys.* **1980**, *58*, 1200, for the nonlocal exchange, nonlocal correlation, and local correlation, respectively.
(25) Becke, A. D. *J. Chem. Phys.* **1993**, *98*, 5648.
(26) Stephens, P. J.; Devlin, F. J.; Chablowski, C. F.; Frisch, M. J. *J. Phys. Chem.* **1994**, *98*, 11623.
(27) Frisch, M. J.; Trucks, G. W.; Schlegel, H. B.; Gill, P. M. W.; Johnson, B. G.; Robb, M. A.; Cheeseman, J. R.; Keith, T.; Petersson, G. A.; Montgomery, J. A.; Raghavachari, K.; Al-Laham, M. A.; Zakrzewski, V. G.; Ortiz, J. V.; Foresman, J. B.; Cioslowski, J.; Stefanov, B. B.; Nanayakkara, A.; Challacombe, M.; Peng, C. Y.; Ayala, P. Y.; Chen, W.; Wong, M. W.; Andres, J. L.; Replogle, E. S.; Gomperts, R.; Martin, R. L.; Fox, D. J.; Binkley, J. S.; Defrees, D. J.; Baker, J.; Stewart, J. P.; Head-Gordon, M.; Gonzalez, C.; Pople J. A. *Gaussian 94, Revision B.1*; Gaussian, Inc.: Pittsburgh PA, 1995.
(28) SIRIUS is an MCSCF program written by H. J. Jensen, H. Agren, and J. Olsen; ABACUS is an MCSCF energy derivatives program written by T. Helgaker, H. J. Jensen, P. Jorgensen, J. Olsen, and P. R. Taylor.
(29) Chertihin, G. V.; Andrews, L.; Bauschlicher, C. W., Jr. *J. Phys. Chem. A* **1997**, *101*, 4026.
(30) Frisch, M. J.; Pople, J. A.; Binkley, J. S. *J. Chem. Phys.* **1984**, *80*, 3265, and references therein.
(31) Wachters, A. J. H. *J. Chem. Phys.* **1970**, *52*, 1033.
(32) Hay, P. J. *J. Chem. Phys.* **1977**, *66*, 4377.
(33) Schafer, A.; Huber, C.; Ahlrichs, R. *J. Chem. Phys.* **1994**, *100*, 5829.
(34) Dunning, T. H. *J. Chem. Phys.* **1989**, *90*, 1007.
(35) Kang, H.; Beauchamp, J. L. *J. Phys. Chem.* **1985**, *89*, 3364.
(36) Wang, L.-S. Personal communication, 1996.
(37) Chertihin, G. V.; Andrews, L. *J. Chem. Phys.* **1996**, *105*, 2561.
(38) Chertihin, G. V.; Bare, W. D.; Andrews, L. *J. Phys. Chem. A* **1997**, *101*, 5090; *J. Chem. Phys.* **1997**, *107*, 2798.

(39) Andrews, L.; Chertihin, G. C.; Citra, A.; Neurock, M. *J. Phys. Chem.* **1996**, *100*, 11235.
(40) Moskovits, M.; Di Lella, D. P. *J. Chem. Phys.* **1980**, *73*, 4917.
(41) Leopold, D. G.; Lineberger, W. C. *J. Chem. Phys.* **1986**, *85*, 51.
(42) Noro, T.; Ballard, C.; Palmer, M. H.; Tatewaki, H. *J. Chem. Phys.* **1994**, *100*, 452.
(43) Di Lella, D. P.; Limm, W.; Lipson, R. H.; Moskovits, M.; Taylor, K. V. *J. Chem. Phys.* **1982**, *77*, 5263.
(44) Shim, I.; Gingerich, K. A. *J. Chem. Phys.* **1983**, *78*, 5693.
(45) This, then, suggests that three different $(FeO_2)_2$ isomers were observed: two different structural isomeric $(FeO_2)_2$ species (861.5 and 585.6 cm^{-1}) and rhombic $O(FeO)_2O$ (705.1 cm^{-1}).
(46) See for example: Duschel, G. K.; Nemetz, T. M.; Ball, D. W. *J. Mol. Struct.* **1996**, *384*, 101.